

High-resolution ion mobility measurements for silicon cluster anions and cations

Robert R. Hudgins,^{a)} Motoharu Imai,^{b)} and Martin F. Jarrold
Department of Chemistry, Northwestern University, Evanston, Illinois 60208

Philippe Dugourd
*Laboratoire de Spectrométrie Ionique et Moléculaire, UMR No. 5579, CNRS et Université Lyon I,
43 bd du 11 novembre 1918, 69622 Villeurbanne Cedex, France*

(Received 3 June 1999; accepted 11 August 1999)

High-resolution ion mobility measurements have been performed for silicon cluster anions and cations, Si_n^- and Si_n^+ , $n = 6-55$. New isomers have been resolved for every cluster size larger than Si_{20} . The results for the anions and the cations have the same global features. However, changing the charge often causes a shift in the isomer distribution, or causes new isomers to emerge. For example, the transition from prolate geometries to more-spherical ones is shifted to larger cluster sizes for the anions than for the cations. The mobilities of the anions are systematically smaller than those of the cations, presumably because of differences in the exterior electron densities. © 1999 American Institute of Physics. [S0021-9606(99)01914-5]

INTRODUCTION

An enormous effort has been devoted to elucidating the structures and electronic properties of isolated silicon clusters. The geometries of the small clusters, n up to 7, have been determined by comparison of high-resolution photoelectron,¹ Raman,² and infrared³ spectra to the predictions of *ab initio* calculations. Polarizability measurements, ionization potential measurements, and photoelectron spectroscopy have been used to measure properties of the intermediate-sized clusters.⁴⁻⁶ However, most of the spectra recorded in this size regime are featureless and they have not yielded much structural information. Ion mobility measurements have revealed much of what is known about the growth of intermediate-sized silicon clusters.^{7,8} The mobility of an ion depends on its average collision cross section with a buffer gas, which in turn depends on the ion's geometry. Comparison of measured mobilities to mobilities calculated for geometries derived from *ab initio* calculations suggests that silicon clusters with 10–20 atoms are built by stacking tricapped trigonal prism units.⁹ A structural transformation occurs at around 25 atoms and this was attributed to a change from elongated geometries to more spherical ones. Several different structures have been proposed for silicon clusters with $n > 25$, including “stuffed-fullerene” structures with a core of tetrahedral silicon.¹⁰ Here we present the first high-resolution ion mobility measurements for silicon cluster anions and cations. The previous mobility measurements were only performed for silicon cluster cations and with lower resolution.^{7,8} With the order of magnitude improvement in the resolving power, new isomers have been resolved for all clusters with more than 20 atoms, and for some clusters with

less than 20 atoms. Drift time distributions for the anions and the cations show the same general features. However, in many cases the isomer distribution shifts, or new isomers emerge on changing the charge. We also find that the mobilities of the anions are systematically smaller than those of the cations, presumably because of differences in the exterior electron densities.

EXPERIMENT

Our high-resolution ion mobility apparatus has previously been described in detail.¹¹ A schematic of the apparatus is shown in Fig. 1. The apparatus consists of a source region coupled directly to a 63 cm long drift tube. Silicon clusters are produced by pulsed laser vaporization of a rotated and translated silicon rod. For some experiments, a second pulsed laser beam was directed into the source region shortly after the vaporization laser, in order to anneal the clusters. Ions pass from the source region into the drift tube through an ion gate. The ion gate consists of a cylindrical channel 0.5 cm in diameter and 2.5 cm long. A He buffer gas counterflow of about 900 sccm prevents neutral clusters from entering the drift tube. A uniform electric field of 180 V/cm carries the ions through the ion gate against the buffer gas flow. The drift tube, ion gate and source region contain helium buffer gas at a pressure of around 500 Torr. A uniform electric field is provided in the drift tube by 46 guard rings coupled to a voltage divider. A drift voltage of 10 000 V was employed, which generates a drift field of 158.7 V/cm. The high drift voltage is primarily responsible for the order of magnitude improvement in the resolution achieved here. After traveling through the drift tube, ions exit through a 0.125 mm aperture. The ions are then focused into a quadrupole mass spectrometer, and after mass analysis, they are detected with an off-axis collision dynode and dual microchannel

^{a)}Present address: Biozentrum der Universität Basel, Klingelbergstr. 70, CH-4056 Basel, Switzerland.

^{b)}Present address: National Research Institute for Metals, 1-2-1 Sengen, Tsukuba, Ibaraki 305-0047, Japan.

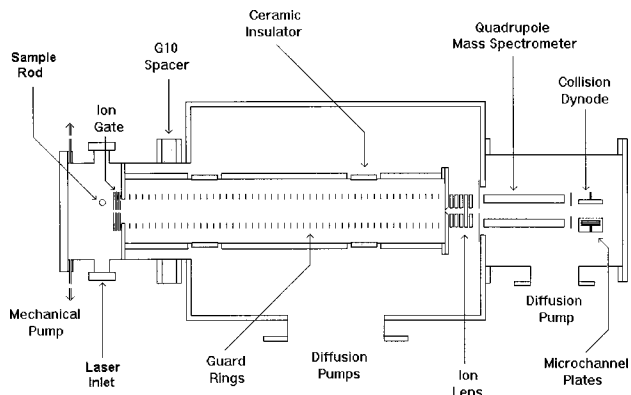


FIG. 1. Schematic diagram of the high-resolution ion mobility apparatus.

plates. Drift time distributions were recorded with a multi-channel analyzer that was synchronized with the laser vaporization pulse.

RESULTS

Figure 2 shows drift time distributions (DTDs) recorded for Si_{10} to Si_{45} anions and cations. The cations are shown on the left and the anions are on the right. Figure 2(a) shows

DTDs for Si_{10} to Si_{21} . A single dominant peak is observed in the distributions for the cations with $n=6-21$. This agrees with the results of previous low-resolution ion mobility measurements for the cations.^{7,8} However, the distributions for some cluster sizes (Si_{17}^+ , Si_{18}^+ , Si_{19}^+ , and Si_{21}^+) have additional, less-intense peaks at either longer or shorter drift times than the dominant peak. This indicates the presence of small amounts of other structural isomers for some of the clusters. For Si_{17}^+ there is a small peak on both sides of the main peak.

Figure 2(b) shows high-resolution DTDs for Si_{22} to Si_{33} . These sizes are in the transition region where previously two isomers were resolved. The previously-recorded low-resolution DTDs for Si_{27}^+ and Si_{28}^+ are compared to the high-resolution results in Fig. 3. It is apparent from this figure that the isomer distributions are similar in the two experiments, although several new isomers are clearly resolved in the present work. The isomers on the right in both scans were previously assigned to prolate geometries, while the isomers on the left were assigned to more-spherical geometries. The transition from prolate to more-spherical geometries was previously observed to start at Si_{24} for the cations.^{7,8} In Fig. 2(b), intensity dramatically shifts from the prolate geometries to the more-spherical ones between Si_{24}^+ and Si_{28}^+ . Thus, the transition occurs for the same cluster sizes despite

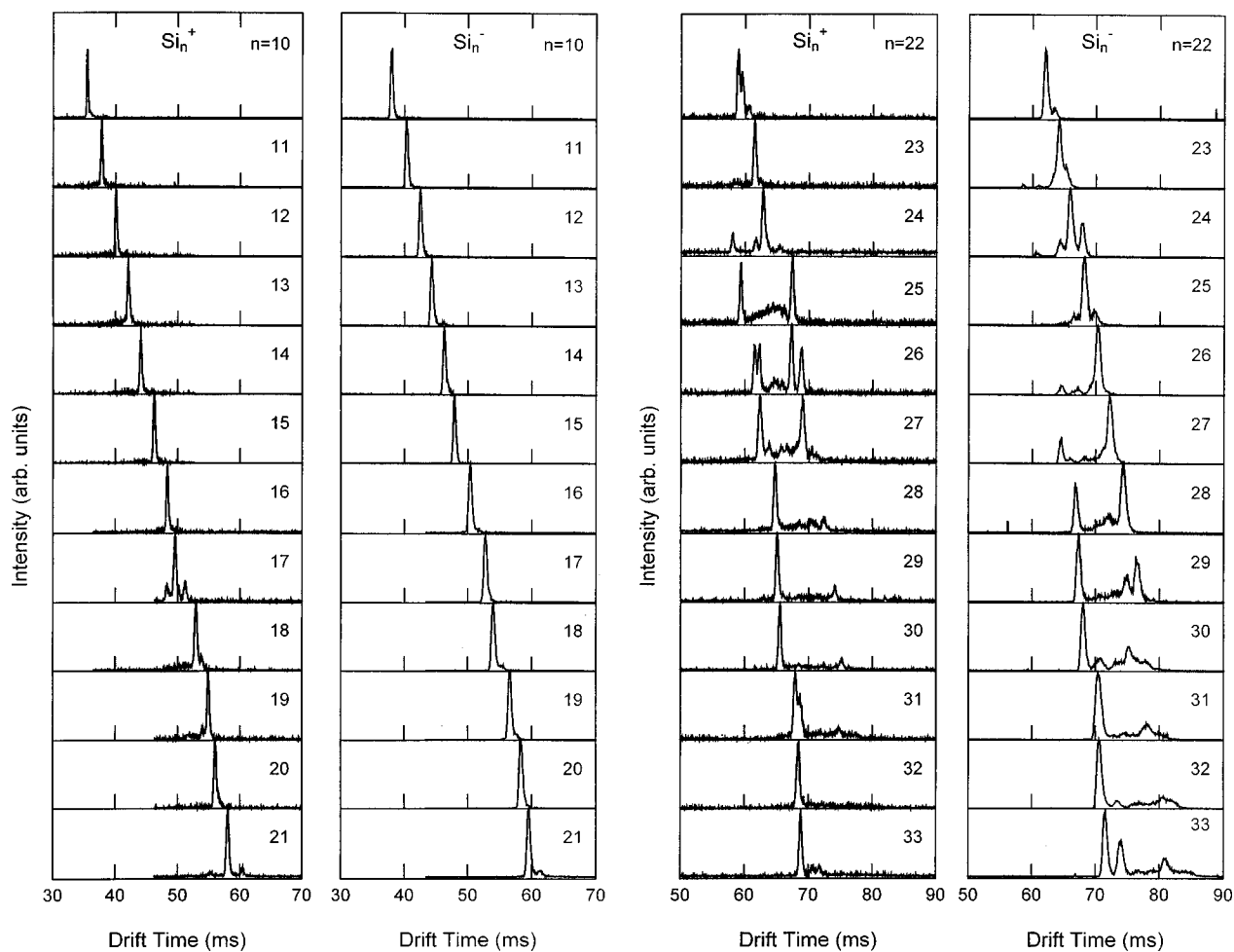


FIG. 2. Drift time distributions (DTDs) of Si_n^+ and Si_n^- , (a) for $n=10-21$, (b) for $n=22-33$, and (c) for $n=34-45$. The DTDs for the cations are on the left and the anions are on the right.

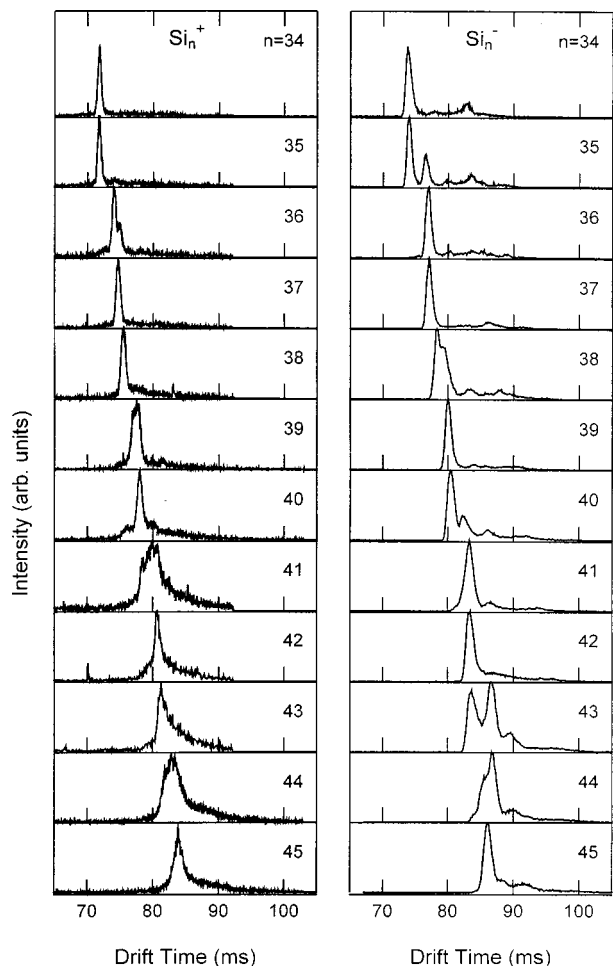
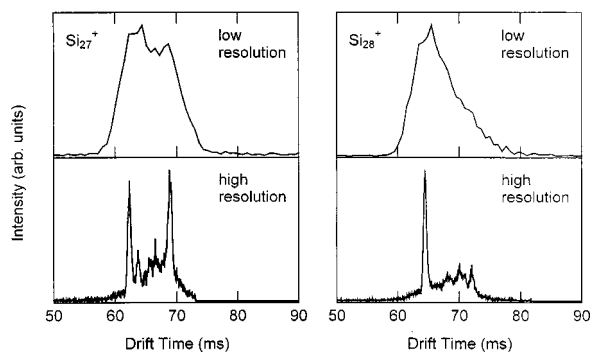


FIG. 2. (Continued.)

the fact that the clusters were prepared under very different conditions. The enhanced resolving power permits the resolution of new isomers throughout the transition region. More than two isomers are clearly resolved for all the cations with 26–33 atoms. For example, for Si_{26}^+ , four sharp, intense peaks are clearly resolved; two in the more-spherical region and two in the prolate region. There are also a number of smaller, less-well-resolved peaks between the two sets of larger peaks. Figure 2(c) shows DTDs for Si_{34} to Si_{45} . For clusters with more than 34 atoms, only a single isomer was

FIG. 3. Drift time distributions for Si_{27}^+ and Si_{28}^+ recorded with the low resolution apparatus and the high-resolution ion mobility apparatus.

resolved in the low resolution ion mobility measurements. Here, multiple isomers are seen for several sizes in this regime. For the larger clusters, in particular, the peaks in the DTDs become very broad. This indicates the presence of several different isomers which are not resolved even with the enhanced resolution.

Drift time distributions for the anions are shown on the right-hand side of Figs. 2(a), 2(b), and 2(c). For the anions a similar structural transformation, from prolate geometries to more spherical ones, occurs in approximately the same size regime as for the cations. The drift times of the anions are systematically shifted to slightly longer times than those for the cations. We will discuss this behavior in more detail below. For anions with 10–21 atoms, Fig. 2(a), there is a single dominant peak in the DTDs. However, there are fewer of the smaller peaks present for the anions than for the cations. For example, only a single dominant peak is present for Si_{17}^- .

For the larger anions, Figs. 2(b) and 2(c), more than two isomers are resolved for each cluster size. The appearance of the DTDs, the number of peaks and their relative intensities, is often very different for the anions and cations. In particular, the structural transformation from prolate to more-spherical that occurs between Si_{24} and Si_{28} for cations, occurs between Si_{26} and Si_{30} for the anions. Although traces of the more-spherical isomer are observed starting from Si_{23}^- . The prolate isomer survives with a significant abundance up to around Si_{38}^- , compared to Si_{31}^+ for cations. Starting at around Si_{40}^- , a broad feature is observed to the right of the dominant peak in the DTDs. This peak is resolved in the DTDs for anions with up to at least 55 atoms. The analog of this peak is identifiable in the DTDs of only a few of the larger cations.

The reduced mobility, K_0 , of an isomer is obtained from its drift time using¹²

$$K_0 = \frac{p}{760} \frac{273.2}{T} \frac{L^2}{t_D V}, \quad (1)$$

where T is the drift tube temperature, p is the buffer gas pressure, L is the length of the drift tube, V is the drift voltage, and t_D is the drift time. Inverse reduced mobilities (which are proportional to the collision cross sections) are plotted in Figs. 4(a) and 4(b) for cations and anions, respectively. Only clearly resolved peaks are reported in these plots. The filled points correspond to the inverse mobility of the dominant isomer for each cluster size. The prolate to more-spherical transition can be clearly seen in these plots. As already mentioned, the prolate isomer survives over a broader size range for anions than for cations. The transition from prolate to more-spherical is not a clean, sharp transformation from one shape to another; a series of intermediate geometries are also present.

The inverse mobilities of the most abundant more-spherical isomers do not increase smoothly. For negatively charged clusters, steps are present in the inverse mobilities of the most abundant isomers after clusters with 30, 33, 35, 38, 40, 43, 46, 49, 51, and 54 atoms (see Fig. 4). For positively charged clusters, the steps are not so well defined. However steps can be identified after clusters with 27, 30, 33, 35, 38,

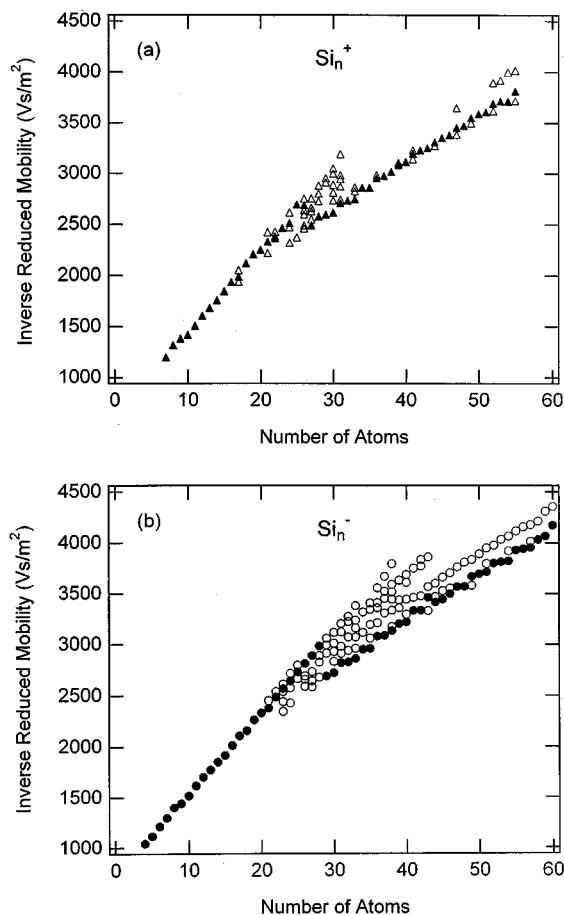


FIG. 4. Plot of inverse reduced mobilities versus number of atoms for Si_n^+ and Si_n^- . The filled points correspond to the most abundant peak observed for each cluster size while additional isomers are shown as open points.

41, 44, 47, 49, 52, and 55 atoms. A step typically occurs every third atom. The steps often overlap. For example, the isomer on the left of the DTD for Si_{43}^- has a mobility almost equal to the mobilities of the main peak for Si_{41}^- and Si_{42}^- , while the other major Si_{43}^- isomer has a mobility almost equal to those for the main peak of Si_{44}^- , Si_{45}^- , and Si_{46}^- . The same type of overlap is also clearly present for Si_{33}^- and Si_{35}^- . The steps do not always appear at the same sizes for anions and cations; for the larger clusters, the steps for cations appear to be shifted up by one atom from those of the anions.

A second family of isomers is resolved as a broad feature at longer drift times than the dominant peak for every cluster anion larger than $n \sim 42$. The increase in inverse mobility for this family of isomers, measured from the center of the broad distribution, is monotonic (see Fig. 4). The peaks for this family of isomers are broader than expected for a single isomer, suggesting that there may be several closely related isomers present for each cluster size. We attempted to anneal the cluster anions with a second XeCl excimer laser directed into the source region soon (~ 1 ms) after the vaporization pulse. DTDs measured for Si_{47}^- with and without annealing are shown in Fig. 5. The intensity of the small peak at longer drift time decreases when the clusters are annealed with the laser. This suggests that the isomers with the shorter drift times are the most stable. However, these

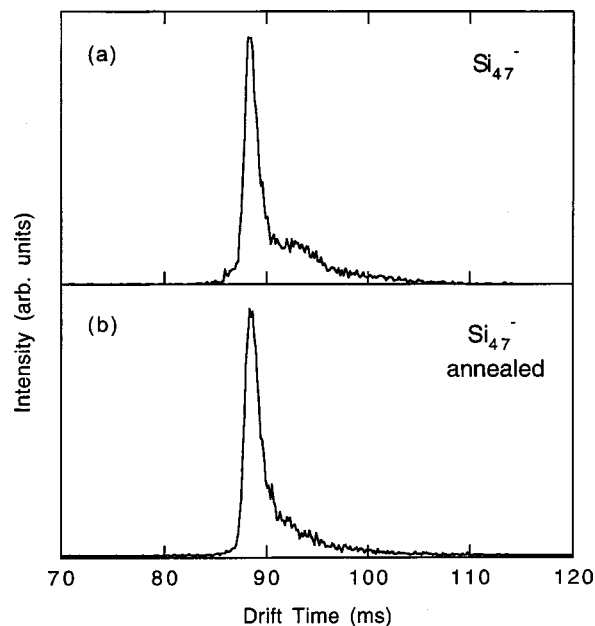


FIG. 5. DTD measured for Si_{47}^- without and with laser annealing.

results could be influenced by other processes such as selective photodetachment or selective photodissociation and so they are not definitive.

It is apparent from Fig. 2 that there is a systematic shift of around 3–4 ms between the main features in the DTDs of the anions and the cations. The anions have systematically longer drift times and hence smaller mobilities than the cations. This indicates that the anions are effectively larger than the cations. The differences between the inverse mobilities of the most intense peak in the DTDs of the anions and cations are plotted in Fig. 6. The average difference is around 100 V s m^{-2} . There are large local fluctuations, which probably result from the change in the charge causing a change in geometry. However, note that we have shown the difference

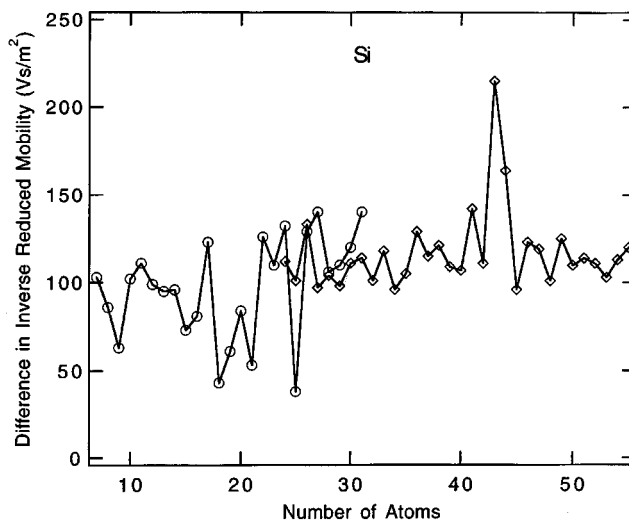


FIG. 6. Plot of the difference between the inverse reduced mobilities of silicon cluster anions and cations. Results are shown for the most intense peak in the DTDs. The circles are for the prolate isomer and the diamonds are for the more-spherical one.

in inverse mobility for the most intense peaks. For some cases, for example the prolate isomers of Si_{17} and Si_{25} , the local fluctuation seems to be due to this choice; if a less-intense adjacent peak is used, the local fluctuation disappears. This observation is consistent with the change in the charge causing a reordering of the low energy isomers of some of the clusters. Si_{43} provides perhaps the most striking example of this behavior.

DISCUSSION

Many new features have been observed with the enhanced resolution available in these experiments. First, we have observed isomers for some of the smaller silicon cluster cations (Si_{17}^+ , Si_{18}^+ , Si_{19}^+ , and Si_{21}^+). Two new isomers were resolved for Si_{17}^+ . Second, in the transition region from Si_{24} up to Si_{30} – Si_{40} , we have resolved numerous new isomers. This observation is consistent with the results of previous chemical reactivity experiments^{13–15} and simultaneous mobility and chemical reactivity measurements,⁸ which indicated the existence of more isomers than revealed in the low-resolution ion mobility measurements. For some cluster sizes, more than six isomers are resolved in the high-resolution DTDs. The wide variety of different structural isomers that apparently coexist may provide an explanation for why it has been difficult to obtain well-defined experimental results, and agreement in the theoretical community about silicon clusters in this size regime. The steps in the mobilities of the larger silicon cluster anions and cations were not observed in the previous low resolution measurements. The steps presumably reflect the growth pattern of silicon clusters in this size regime, and they should emerge from theoretical predictions of the structures of these species.

The results in Figs. 2(a), 2(b), and 2(c) clearly show that the charge state affects the relative stability of the different isomers, even for quite large clusters. The transition between prolate and more-spherical geometries occurs earlier for cations than for anions. The prolate geometries persist for larger cluster sizes for the anions than for the cations. Apparently, the two extra electrons in the anions stabilize the prolate isomers relative to the more-spherical ones. Changing the charge also causes a shift in some of the mobility steps observed for larger cluster sizes. Structural changes caused by charging neutral silicon clusters have previously been examined in theoretical studies.^{16,17} R othlisberger and collaborators¹⁰ have reported that there are a wealth of slightly different Si_{45} isomers within 0.1 eV/atom of one another. So it is not surprising that changing the charge can cause changes in the relative stabilities of some of the isomers.

As noted above there is a systematic shift in the mobilities of the silicon cluster anions and cations. It is unreasonable to assign this shift (that is observed for every cluster size) to a structural change. We recently reported mobilities measured for indium cluster anions and cations.¹⁸ A systematic difference between the mobilities of the anions and cations was also observed for these clusters, and was attributed to the extra charge causing the surface electron density of the anions to spill-out further than for the cations. It seems likely

that this explanation can also account for the systematic difference in the mobilities of the silicon cluster anions and cations. For indium clusters the difference between the mobilities of the anions and cations decreases with increasing cluster size (from around 100 to 200 V s m^{-2} for dimers, trimers, and tetramers to around 50 V s m^{-2} for In_{30}). The differences in the mobilities of the indium cluster anions and cations are in agreement with the predictions of a simple model based on the spill-out of the electron density from jellium spheres. We have also examined the difference between the mobilities of fullerene anions and cations with 60–100 carbon atoms. Here the difference between the mobilities of the anions and cations is much smaller, ranging from around 17 V s m^{-2} for C_{60} to around 0 V s m^{-2} for C_{100} . The small difference between the mobilities of the fullerene anions and cations suggests that the extra electrons go into orbitals which do not lead to a substantial increase in the exterior electron density. For the silicon clusters, the difference between the mobilities of the anions and cations is comparable to that found for the indium clusters, except that the difference does not decline with increasing cluster size. This suggests that the extra electrons are mainly localized on the cluster surface, where they effectively add a constant volume to the cluster.

CONCLUSIONS

High-resolution ion mobility measurements have been performed for Si_n cluster anions and cations with $n = 6$ – 55 . New isomers have been resolved for almost every cluster size larger than Si_{16} . Changing the charge often induces a structural change by changing the relative energies of the different isomers. In particular, the addition of two electrons increases the relative stability of the prolate isomers relative to the more-spherical ones, so that the structural transition from prolate to more spherical occurs later for anions than for cations. The inverse mobilities of the anions are systematically larger than those of the cations. This shift results from differences in the exterior electron density caused by the addition of the extra electrons.

ACKNOWLEDGMENTS

This work was partially supported by the National Science Foundation (CHE-9618643) and NATO (CRG-971066). M. Imai thanks The Science and Technology Agency in Japan and The National Research Institute for Metals for their financial support.

¹C. S. Xu, T. R. Taylor, G. R. Burton, and D. M. Neumark, *J. Chem. Phys.* **108**, 1395–1406 (1998).

²E. C. Honea, A. Ogura, C. A. Murray, K. Raghavachari, W. O. Sprenger, M. F. Jarrold, and W. L. Brown, *Nature (London)* **366**, 42–44 (1993).

³S. Li, R. J. Van Zee, W. Weltner, and K. Raghavachari, *Chem. Phys. Lett.* **243**, 275–280 (1995).

⁴J. Woenckhaus, R. Sch afer, and J. A. Becker, *Surf. Rev. Lett.* **3**, 371–375 (1996).

⁵K. Fuke, K. Tsukamoto, F. Misaizu, and M. Sanekata, *J. Chem. Phys.* **99**, 7807–7812 (1993).

⁶O. Cheshnovsky, S. H. Yang, C. L. Pettiette, M. J. Craycraft, Y. Liu, and R. E. Smalley, *Chem. Phys. Lett.* **138**, 119–124 (1987).

⁷M. F. Jarrold and V. A. Constant, *Phys. Rev. Lett.* **67**, 2994–2997 (1991).

⁸M. F. Jarrold and J. E. Bower, *J. Chem. Phys.* **96**, 9180–9190 (1992).

- ⁹K.-M. Ho, A. A. Shvartsburg, B. C. Pan, Z. Y. Lu, C. Z. Wang, J. G. Wacker, J. L. Fye, and M. F. Jarrold, *Nature (London)* **392**, 582–585 (1998).
- ¹⁰U. Röthlisberger, W. Andreoni, and M. Parrinello, *Phys. Rev. Lett.* **72**, 665–668 (1994).
- ¹¹P. Dugourd, R. R. Hudgins, D. E. Clemmer, and M. F. Jarrold, *Rev. Sci. Instrum.* **68**, 1122–1129 (1997).
- ¹²E. A. Mason and E. W. McDaniel, *Transport Properties of Ions in Gases* (Wiley, New York, 1988).
- ¹³K. M. Creegan and M. F. Jarrold, *J. Am. Chem. Soc.* **112**, 3768–3773 (1990).
- ¹⁴S. Maruyama, L. R. Anderson, and R. E. Smalley, *J. Chem. Phys.* **93**, 5349–5351 (1990).
- ¹⁵J. M. Alford, R. T. Laaksonen, and R. E. Smalley, *J. Chem. Phys.* **94**, 2618–2630 (1991).
- ¹⁶J. R. Chelikowsky and N. Binggeli, *Mater. Sci. Forum* **232**, 87–102 (1996).
- ¹⁷B. Liu, A. A. Shvartsburg, Z.-Y. Lu, B. Pan, C.-Z. Wang, K.-M. Ho, and M. F. Jarrold, *J. Chem. Phys.* **109**, 9401–9409 (1998).
- ¹⁸J. Lermé, P. Dugourd, R. R. Hudgins, and M. F. Jarrold, *Chem. Phys. Lett.* **304**, 19–22 (1999).